Journal of the Geological Society, London, Vol. **163**, 2006, pp. 539–547. Printed in Great Britain.

Late Carboniferous plutonism within the pre-Alpine basement of the External Hellenides (Kithira, Greece): evidence from U–Pb zircon dating

P. XYPOLIAS[1], W. DÖRR[2] & G. ZULAUF[3]

[1]*Department of Geology, University of Patras, GR-26500, Patras, Greece (e-mail: p.xypolias@upatras.gr)*

[2]*Institut für Geowissenschaften und Lithosphärenforschung, Justus-Liebing Universität, Senkenbergstr. 3, D-35390, Giessen, Germany*

[3]*Geologisch–Palaeontologisches Institut, Universität Frankfurt a.M., Senckenberganlage 32–34, D-60054, Frankfurt a.M., Germany*

In memory of Theodor Doutsos, for his invaluable contribution to the understanding of geology of Greece

Abstract: U–Pb zircon dating of three granitic orthogneisses, sampled from Kithira island, SW Greece, provide the first reliable evidence for Carboniferous plutonism within the pre-Alpine basement of the External Hellenides. Concordant zircons from two samples yielded ages at 324 ± 2 Ma and 323 ±3 Ma, whereas the third sample yielded a lower intercept age at 320 ± 1.2 Ma. The concordant ages are interpreted to date the emplacement of the igneous protolith. Ages of inherited zircons of two orthogneisses range from 2.5 to 2.4 Ga, indicating Late Archaean–Early Proterozoic crustal components. In combination with published ages for other Aegean metagranitoids, the new U–Pb ages provide additional evidence of a temporally restricted period of plutonism in the pre-Alpine Aegean region from 325 to 300 Ma. Comparing the post-Neoproterozoic evolution of the investigated basement with that of the Cycladic and Pelagonian basements and of the continental massifs of NE Greece and Turkey, we argue that all these crustal blocks were part of the Gondwana-derived Cimmerian terrane. Based on the spatial and temporal distribution of Late Carboniferous Aegean plutonism, we suggest that this period of magmatic events results from the southward subduction of Palaeotethys beneath the marginal fragments of northern Gondwana.

In late Palaeozoic time, a large Tethyan Ocean (Palaeotethys), narrowing to the west, existed between Gondwana and Eurasia (e.g. Robertson *et al*. 1991). In this palaeogeographical setting, the pre-Alpine basement of the External Hellenides has been argued by many workers to be part of the Apulia (or Adria) microcontinent, which was situated at the northern margin of Gondwana (e.g. Robertson & Dixon 1984; Şengör *et al*. 1984; Dercourt *et al*. 1986; Robertson *et al*. 1996; Stampfli & Mosar 1999). However, there is no consensus on the precise relative position of Apulia and adjacent continental fragments (e.g. the Menderes and Cycladic massifs; Fig. 1) at the margin of Gondwana (e.g. Robertson *et al*. 1996; Ring *et al*. 1999*a*; Stampfli 2000). Moreover, the timing of separation of these microcontinents from Gondwana is still a matter of debate. Various models, based principally on lithostatigraphy, have been proposed dealing with this problem. One popular concept invokes rifting of Apulia from the northern margin of Gondwana during Late Triassic–Jurassic times and independent drifting of the microcontinent toward the NE throughout the Mesozoic (e.g. Robertson *et al*. 1991, 1996). Other investigators have suggested that a part of the pre-Alpine basement of the External Hellenides belonged to the western termination of the Cimmerian superterrane (Stampfli & Mosar 1999; Stampfli & Borel 2002), a terrane that rifted away from the northeastern Afro-Arabian margin after the Late Carboniferous, drifted toward the north and entered into collision with the southern Eurasian margin during Permo-Triassic times. A third model suggests Permo-Triassic rifting of Cimmerian fragments (e.g. Taurides, Sakarya and Rhodope; Fig. 1) coeval with southward subduction of the Palaeotethyan ocean beneath northern Gondwana (Şengör *et al*. 1984).

Major reasons for this poorly constrained and controversial evolution of the pre-Alpine basement of the External Hellenides are the lack of reliable age data and the limited exposures of basement rocks. Until now, remnants of the basement rocks have been found only in Crete and the Dodecanese (Seidel 1978; Franz 1992; Romano *et al*. 2004). They consist of gneiss, micaschist, amphibolite and marble. Based on K–Ar cooling ages of muscovite and hornblende, the metamorphism of these rocks was assumed to be 'Variscan' (Seidel *et al*. 1982). However, recent U–Th–Pb dating of monazite and U–Pb dating of zircon from basement slices of eastern Crete (Fig. 1) revealed a more complex evolution of the pre-Alpine basement of the External Hellenides. These data suggest an igneous event during Cambrian times (*c*. 510 Ma), two distinct metamorphic events in the Carboniferous (*c*. 330 Ma) and Permian (*c*. 260 Ma), and a Triassic igneous event (*c*. 223 Ma) (Finger *et al*. 2002; Romano *et al*. 2004). In this study, we present new U–Pb zircon ages from orthogneisses of the pre-Alpine basement of Kithira island (External Hellenides; Fig. 1), which document an additional igneous event in the Carboniferous. We compare the new zircon ages with published geochronological data from other basement rocks of the Aegean region and discuss the origin and evolution of the investigated crustal block within the Tethyan framework.

Regional geological setting

As a part of the Alpine orogenic belt, the External Hellenides are forming an orocline that connects the Dinarides to the NW with the Taurides to the SE (Fig. 1). The External Hellenides mainly consist of Meso- and Cenozoic sedimentary rocks that were deposited on top of the rifted margin of the Apulia microconti-

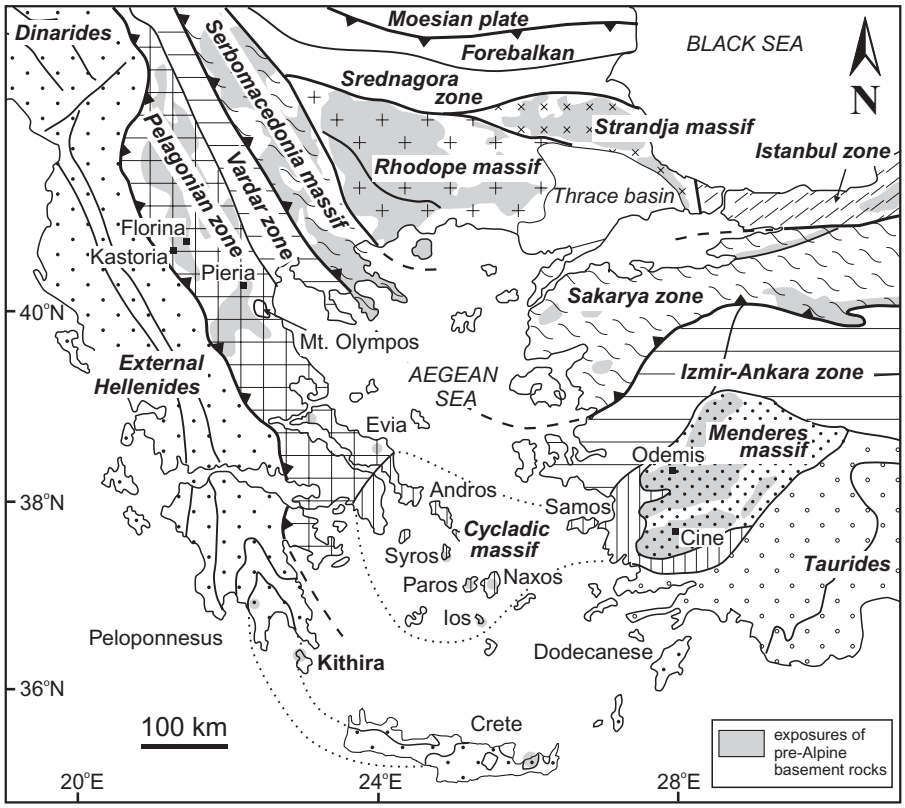

Fig. 1. Sketch map of major tectonic elements in the southern Balkan peninsula and western Turkey.

nent. The present sequence of the pre-Neogene nappes of the External Hellenides results from northward Cenozoic subduction and collision between Apulia and the Pelagonian microcontinent (Mountrakis 1986; Robertson *et al*. 1991; Doutsos *et al*. 1993).

There are three main tectonostratigraphic units on Kithira island: the Pindos unit, the Tripolitza unit and the Phyllite–Quartzite unit. The non-metamorphic Pindos and Tripolitza units represent the uppermost structural units in the study area. These units are composed of Triassic to Eocene carbonate rocks and an upper Eocene flysch. On Peloponnesus and Crete (Fig. 2a), a thin anchimetamorphosed Permo-Triassic sequence, referred to as the Tyros and Ravdoucha Beds, respectively, is present at the base of the Tripolitza carbonates. The high-pressure metamorphic rocks of the Phyllite–Quartzite unit largely consist of phyllites, quartzites, metaconglomerates and metavolcanic rocks, with local marble intercalations. The protolith of the Phyllite–Quartzite unit has been considered as a mid-Carboniferous to Triassic rift sequence (Krahl *et al*. 1983) that accumulated during the opening of a southern Neotethyan strand (Pe-Piper 1982; Seidel *et al*. 1982; Robertson & Dixon 1984). The basement of the sequence is generally not exposed; however, several relic slices of pre-Alpine crystalline rocks have been identified within the Phyllite–Quartzite unit, especially on Crete. During Late Oligocene–Early Miocene times the protolith of the Phyllite–Quartzite unit underwent HP metamorphism (Seidel *et al*. 1982) in the course of intracontinental subduction within the Apulian crust (Xypolias

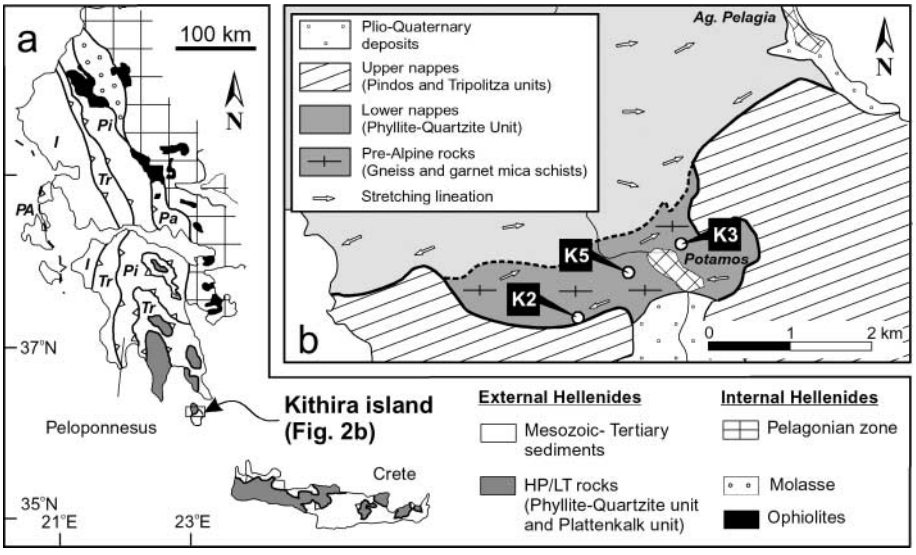

Fig. 2. (**a**) Geological map of the southwestern Hellenides showing major tectonostratigraphic units. PA, Pre-Apulia zone; I, Ionian zone; Tr: Tripolitza zone; Pi, Pindos zone; Pa, Parnassos zone. (**b**) Geological map from northern Kithira showing the exposure of the pre-Alpine rocks, the orientation of the main stretching lineation, and the locations of samples that were collected for U–Pb zircon dating.

& Doutsos 2000; Xypolias & Koukouvelas 2001). Peak P–T conditions of this metamorphism for the rocks exposed on Kithira and southern Peloponnesus are estimated at 450 ± 30 °C and 13–17 kbar (e.g. Theye *et al*. 1992).

Field mapping on Kithira has revealed a pre-Alpine crystalline basement that is well exposed around Potamos village, covering an area of *c*. 5 km^2 (Fig. 2b). Basement rocks constitute a crystalline complex of orthogneiss, paragneiss, and garnet–mica schists with local marble intercalations. They are mainly incorporated within the upper structural levels of the Phyllite–Quartzite unit and also appear to be in tectonic contact with the Tripolitza and Pindos units. In the study area the contact between gneisses and metasedimentary rocks of the Phyllite–Quartzite unit is strongly modified by shearing and folding. Blue amphibole in paragneiss suggests that these basement rocks have been affected by the Alpine HP–LT metamorphism. Moreover, an ENE–WSW-trending stretching lineation within gneiss is defined by the shape-preferred orientation of feldspar and quartz. This lineation is subparallel to the stretching lineation within the Phyllite–Quartzite unit (Fig. 2b).

Sample description

For the purposes of the present study we collected three felsic orthogneiss samples (Figs 2b and 3a). Sample K2 was collected from a road cut *c*. 1300 m SW of Potamos village. Sample K3 was collected from a road cut at the northern margin of Potamos, behind the home for the aged. Sample K5 was collected from a path cut *c*. 500 m west of Potamos.

All samples are composed of quartz, K-feldspar, plagioclase and muscovite as essential minerals, with epidote, zoisite, apatite and zircon as accessories. The quartz grains show evidence of dynamic recrystallization and subgrain formation (Fig. 3b). The subgrain boundaries are aligned parallel to the prism planes. Recrystallization has been accommodated by both low-temperature grain-boundary migration and subgrain rotation. No evidence was found for crystal-plastic deformation of feldspars, which often occur as rigid porphyroclasts (Fig. 3c). The asymmetric shape of these clasts as well as asymmetric pressure shadows of recrystallized quartz behind feldspar indicate a top-to-the-west sense of shear (Fig. 3d and e). In samples K2 and K3 a well-developed foliation results from the shape-preferred orientation of mica, quartz ribbons and feldspar (Fig. 3a). In sample K5 the feldspar porphyroclasts are surrounded by a schistose matrix of mica and dynamically recrystallized aggregates of quartz forming ‘core and mantle’ structures (Fig. 3c). Fluid activity is documented in all samples by sericitization of feldspar and the precipitation of hydrothermal minerals along cracks or veins.

Analytical methods

Zircons of the three samples were separated and analysed at the Justus-Liebig-Universität Giessen. After removal of the weathered surfaces, the samples, each *c*. 30 kg, were crushed, pulverized and processed on a Wilfley table to extract concentrates of heavy minerals. Further separation of the heavy mineral fractions was achieved using the heavy liquid density contrast technique and a Frantz isodynamic separator. Finally, zircons were hand-picked under a binocular microscope. Only inclusion-free zircons were selected for isotopic analyses. The internal structure of zircons was investigated by cathodoluminescence (CL) imaging, using a JEOL Superprobe JXA-8900 at the Universität Frankfurt, operating at a voltage of 15 kV and current of 2.3–3.7 nA.

The zircons were abraded for 6–24 h with pyrite and washed with

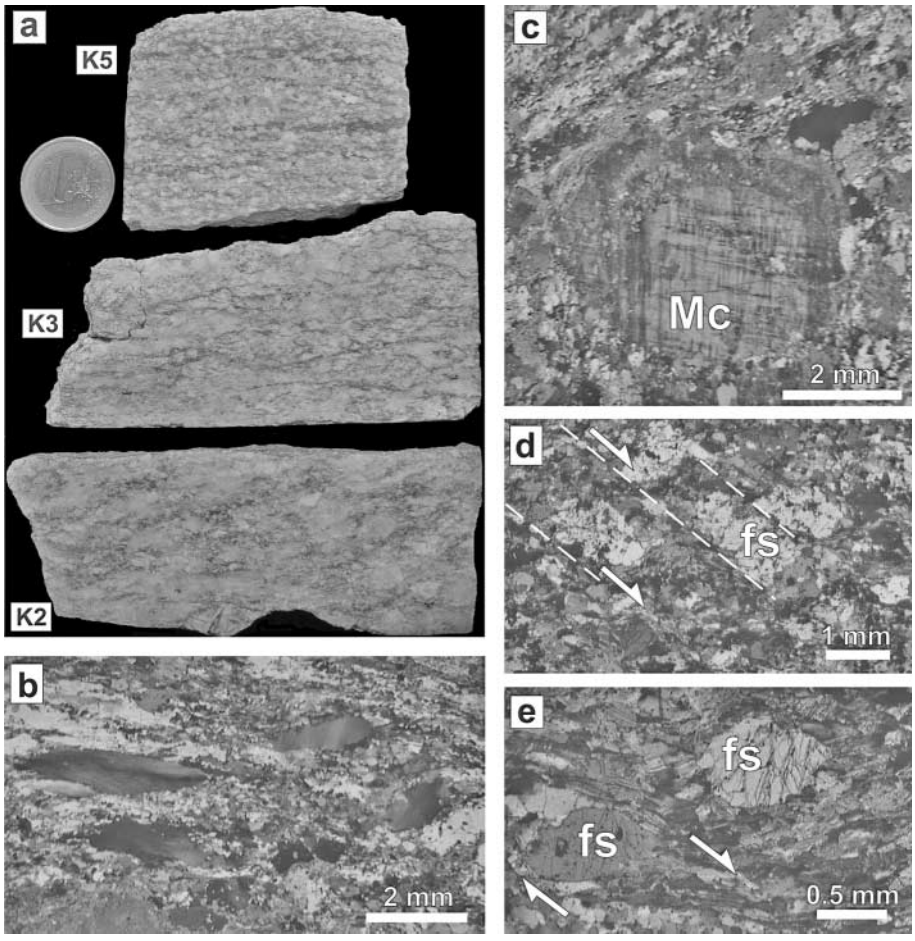

Fig. 3. (**a**) Hand specimens of the dated orthogneiss samples. Foliation of samples K2 and K3 results from shape-preferred orientation of mica, quartz and feldspar. Feldspar porphyroclasts of sample K5 are wrapped by a schistose matrix of mica and quartz. (**b**) Photomicrograph (cross-polarized light) of orthogneiss K2. The quartz grains show evidence for dynamic recrystallization and subgrain formation. (**c**) Photomicrograph (cross-polarized light) of orthogneiss K5 showing almost undeformed microcline porphyroclasts (Mc) within a more ductile fine-grained matrix. (**d**,**e**) Photomicrograph (cross-polarized light) of orthogneiss K2. The asymmetric shape of feldspar (fs) as well as asymmetric pressure shadows of recrystallized quartz behind feldspar indicate a top-to-the-west sense of shear.

HNO_3 and 2 N HCl in an ultrasonic basin. Dissolution and separation of U and Pb were carried out following the technique of Krogh (1973). Zircons were dissolved and spiked using a ^{235}U–^{205}Pb tracer. The U–Pb separation was carried out with 80 µl columns containing an ion-exchange resin (Bio-Rad, AG 1×8, 100–200 mesh) in a stepwise elution process.

The separated U and Pb were loaded on single Re filaments. Isotopic composition was measured using isotope dilution thermal ionization mass spectrometry (Finnegan MAT 261, see also Dörr *et al*. 2002). The beam intensities of ^{207}Pb and ^{206}Pb allowed static mode measurement with 2σ errors typically less than 1‰. The measured Pb isotopic ratios were corrected for mass fractionation (1.12 ± 0.18‰ per a.m.u.), blank and initial Pb. Pb blanks were *c*. 3–5 pg. The calculation and correlation of uncertainties for $^{206}Pb/^{238}U$ and $^{207}Pb/^{235}U$ were carried out after Ludwig (1980) using the program PbDat (Ludwig 1988). Ages were calculated using the decay constants of Jaffey *et al*. (1971) and Steiger & Jäger (1977). Regression lines and concordia diagrams were constructed using the program Isoplot (Ludwig 2001).

Results

Morphology and CL characteristics of zircons

Zircons extracted from three orthogneisses are pinkish to colourless and form 250–350 µm long prismatic, euhedral crystals with aspect ratios of 3–4. According to the typological classification of Pupin (1980), the zircon crystals predominantly belong to subtypes G_1 to $L_{2/3}$ and, to a lesser extent, to subtypes L_5, $S_{6/7}$ and S_{12}. On the base of CL imagery, the majority of analysed zircons exhibit fine oscillatory growth zonation and the absence of inherited component (Fig. 4a, b, d and e) suggesting comagmatic crystallization (e.g. Corfu *et al*. 2003). Oscillatory zoning texture is characterized by dark to bright colours and sometimes interrupted by thin dark layers. The bright colours represent more or less pure zircon phase whereas the dark colours reflect variable U and Y contents. Generally, the zircon growth starts with P-type zircon faces, which were overgrown by (211) pyramid faces of S-type zircons. The outer parts of the zircons are built up by dark prisms and pyramids (Fig. 4a and d). CL imaging of some zircons from orthogneiss K3 indicates the presence of xenocrystal cores. As illustrated in Figure 4c, the zircon grain contains a rounded heterogeneous dark core, which is surrounded by a discordant bright zone indicating inheritance and dissolution. According to Poller *et al*. (1997), such composite grains should both provide age information and constrain a discordia line with inherited upper and magmatic lower intercept ages.

U–Pb dating of zircons

The results of the U–Pb isotope analyses of zircons from the three orthogneisses are listed in Table 1 and summarized in concordia diagrams (Figs 5–7). The uncertainties of individual data points are shown by 2σ ellipses.

Orthogneiss K2. One zircon is concordant at 324 ± 2 Ma (2 in Fig. 5) and four other single zircons plot close to the concordia curve at 325 Ma (3, 5, 6 and 7 in Fig. 5). The 324 ± 2 Ma age of the concordant zircon (zircon 2) is interpreted to reflect the time of crystallization of the igneous protolith of orthogneiss K2.

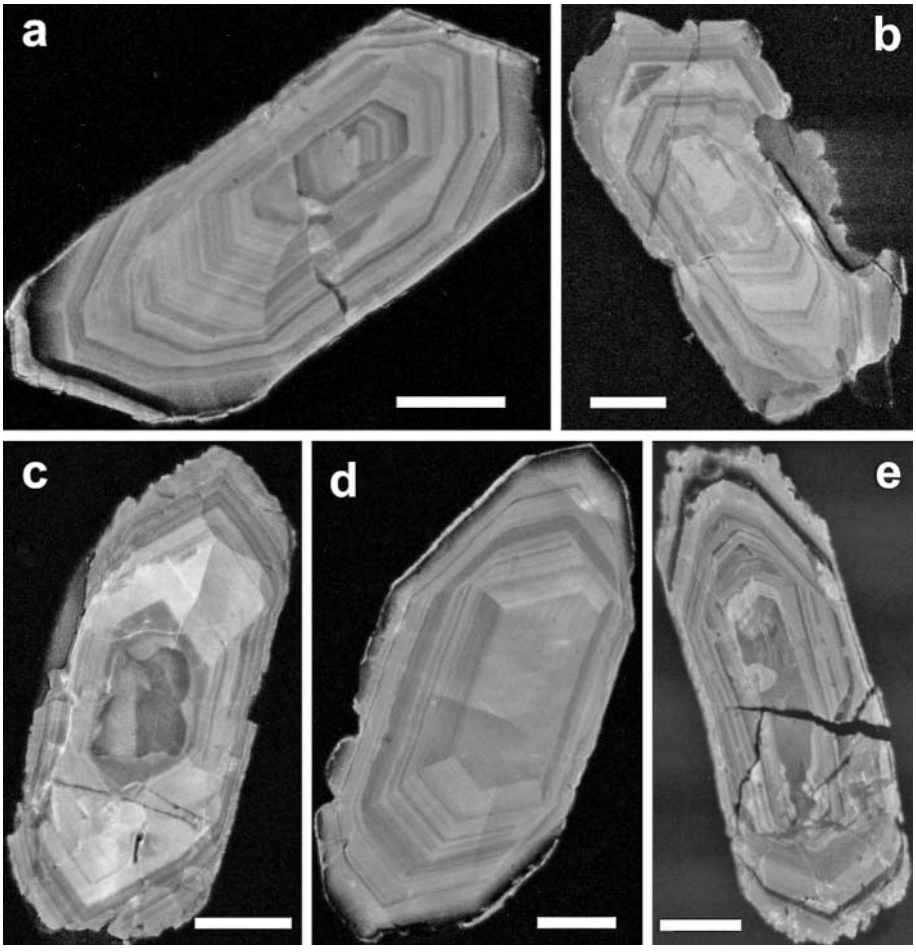

Fig. 4. Cathodoluminescence (CL) images of comagmatic zircon crystals from orthogneiss samples: (**a**, **b**) K2; (**c**, **d**) K3; (**e**) K5. Images oriented parallel to the zircon *c*-axis. The scale bar represents 50 µm in all images.

Table 1. *U–Pb isotope analyses of zircons from Kithira orthogneiss*

Sample	Weight (μg)	Concentrations			Atomic ratios				Cor.	Apparent ages (Ma)		
		U (ppm)	Pb r. (ppm)	Pb i. (ppm)	$^{206}Pb/^{204}Pb^*$	$^{207}Pb/^{235}U \pm 2\sigma$	$^{206}Pb/^{238}U \pm 2\sigma$	$^{207}Pb/^{206}Pb \pm 2\sigma$		$^{206}Pb/^{238}U$	$^{207}Pb/^{235}U$	$^{207}Pb/^{206}Pb$
K2												
1	16	350	18.1	2.94	415	0.4269 ± 0.84	0.05350 ± 0.51	0.05787 ± 0.63	0.66	336 ± 2	361 ± 3	525 ± 14
2	21	354	17.3	1.67	700	0.3761 ± 0.84	0.05154 ± 0.42	0.05293 ± 0.71	0.53	324 ± 1	324 ± 3	325 ± 16
3	14	298	14.1	1.16	840	0.3912 ± 1.65	0.05073 ± 0.76	0.05593 ± 1.45	0.48	319 ± 3	335 ± 6	449 ± 32
4	14	152	7.6	1.77	300	0.4177 ± 2.00	0.05188 ± 1.35	0.05840 ± 1.41	0.71	326 ± 4	354 ± 7	544 ± 31
5	21	293	14.4	0.99	978	0.3808 ± 0.91	0.05162 ± 0.51	0.05350 ± 0.73	0.59	324 ± 2	328 ± 3	350 ± 17
6	17	158	7.7	1.11	474	0.3807 ± 1.90	0.05120 ± 1.12	0.05393 ± 1.49	0.62	322 ± 3	328 ± 6	368 ± 34
7	13	292	14.2	1.00	964	0.3911 ± 1.29	0.05160 ± 0.80	0.05500 ± 0.98	0.65	324 ± 3	335 ± 4	411 ± 22
K3												
8	31	107	5.3	0.39	895	0.3750 ± 1.52	0.05147 ± 0.92	0.05284 ± 1.18	0.63	323 ± 3	323 ± 5	322 ± 27
9	17	396	19.5	0.81	1586	0.3715 ± 0.76	0.05092 ± 0.47	0.05291 ± 0.60	0.64	320 ± 2	321 ± 3	325 ± 14
10	19	302	14.3	0.55	1756	0.3652 ± 0.97	0.05008 ± 0.57	0.05289 ± 0.76	0.62	315 ± 2	316 ± 3	324 ± 17
11	11	273	14.1	2.04	463	0.4079 ± 1.46	0.05274 ± 0.96	0.05609 ± 1.05	0.70	331 ± 3	347 ± 5	456 ± 23
12	27	293	16.5	5.14	216	0.4596 ± 1.06	0.05504 ± 0.36	0.06057 ± 0.96	0.44	345 ± 2	384 ± 4	624 ± 21
K5												
13	34	156	7.7	0.43	1186	0.3763 ± 0.94	0.05112 ± 0.59	0.05338 ± 0.71	0.65	321 ± 2	324 ± 3	345 ± 16
14	21	699	33.1	1.81	1272	0.3857 ± 0.70	0.05152 ± 0.24	0.05431 ± 0.64	0.41	324 ± 1	331 ± 2	384 ± 14
15	19	126	6.4	1.49	291	0.3821 ± 2.06	0.05136 ± 1.21	0.05395 ± 1.60	0.63	323 ± 4	329 ± 6	369 ± 36
16	17	225	39.1	1.96	1181	3.0549 ± 0.45	0.16123 ± 0.42	0.13742 ± 0.15	0.94	964 ± 4	1421 ± 6	2195 ± 3

Pb r., radiogenic lead; Pb i., initial common lead; Cor., correlation coefficient of $^{207}Pb/^{235}U$ to $^{206}Pb/^{238}U$ errors. *Corrected for mass fractionation (1.12 ± 0.18‰ per a.m.u.), ^{205}Pb spike contribution and analytical blank.

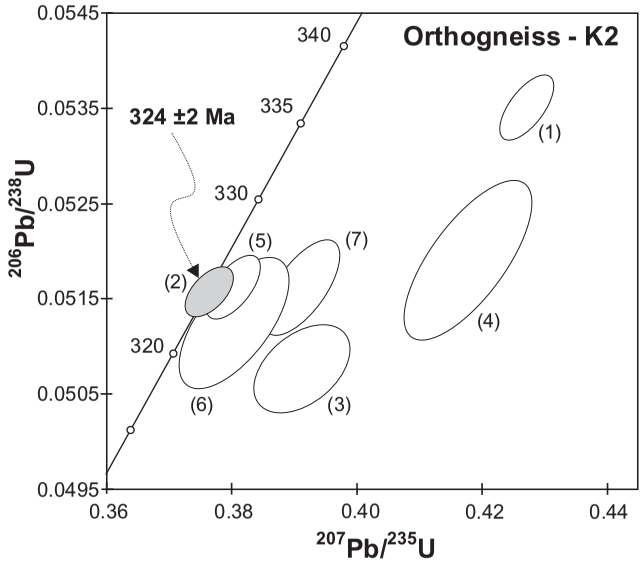

Fig. 5. Concordia diagram for orthogneiss K2. Numbering and error of the ellipses are given in Table 1.

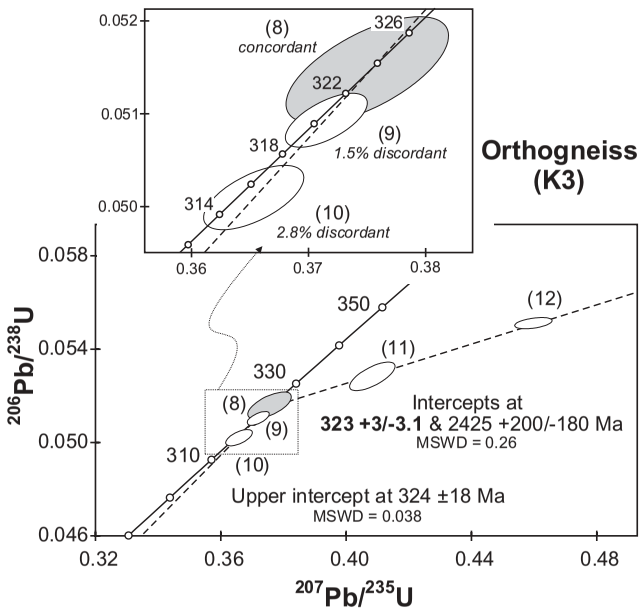

Fig. 6. Concordia diagram for orthogneiss K3. Numbering and error of the ellipses are given in Table 1.

Zircons 5 and 6 touch the concordia curve with their error ellipses. Zircons 1 and 4 point to an inherited component older than 525 Ma (Table 1, Fig. 5).

Orthogneiss K3. Three zircons plot at the concordia curve between 315 and 325 Ma (8, 9 and 10 in Fig. 6), and two zircons are discordant (11 and 12 in Fig. 6). The concordant zircon (8) together with the discordant zircons (11 and 12) define a regression line (MSWD = 0.26) with a lower intercept age at 323 ± 3 Ma and a loosely constrained upper intercept age of 2425 +200/−180 Ma. The upper intercept confirms the presence

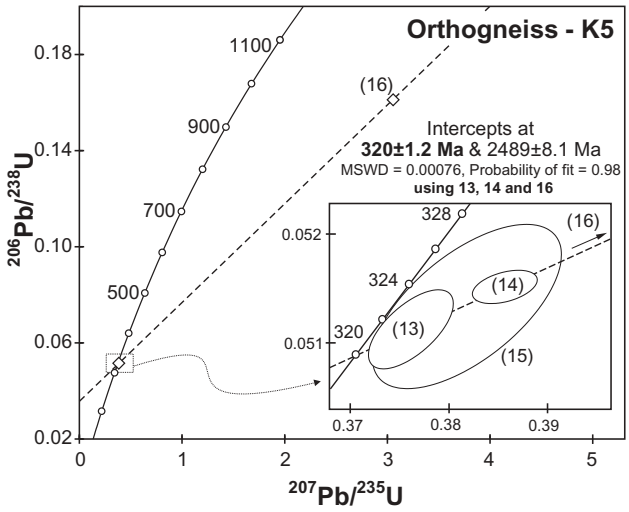

Fig. 7. Concordia diagram for orthogneiss K5. Numbering and error of the ellipses are given in Table 1.

of an inherited Late Archaean–Early Proterozoic component. The concordant zircon (8) and the two subconcordant zircons (9, 1.5% discordant; 10, 2.8% discordant) plot close together and define a discordia (MSWD = 0.038; a short defined discordia with 0.5–1% error of analysis) with an upper intercept age at 324 ± 18 Ma, fixed by concordant zircon, and an ill-defined lower intercept at −24 ± 1200 Ma. This proves that zircons 9 and 10 underwent a later lead loss. The two discordia lines overlap. The Carboniferous granitic magma emplacement age is constrained by a concordant data point at 323 ± 3 Ma.

Orthogneiss K5. The four analysed single zircons (13–16 in Fig. 7) display a typical trend for lead inheritance. Zircon 16 yielded high apparent U–Pb ages with high ^{208}Pb content. Two zircons (13 and 15 in Fig. 7) are nearly concordant and touch the concordia curve with their error ellipses at *c*. 322 Ma. Without zircon 15 (high error), the single zircons 13, 14 and 16 define a discordia (MSWD = 0.00076) with a lower intercept at 320 ± 1.2 Ma and an upper intercept at 2489 ± 8 Ma. A discordia line with nearly the same upper intercept age (2470 Ma) could be also calculated by using only the three points (13, 14 and 15 in Fig. 7) close to the concordia curve. This upper intercept age is *c*. 60 Ma older than the estimated age for orthogneiss K3. We interpret the lower intercept as a minimum age for the intrusion of the protolith. The upper intercept age suggests the main inherited component to be Late Archaean–Early Proterozoic in age.

Discussion

Precambrian records

Inherited zircons from two samples (K3 and K5) analysed in this study yielded upper intercept ages that cluster between 2500 and 2400 Ma, indicating the presence of a Late Archaean–Early Proterozoic crustal component in the pre-Alpine basement of the External Hellenides. Possibly, the inherited zircons result from reworking of this ancient crustal material during Carboniferous melting and magma formation. Similar *c*. 2500–2450 Ma ages have been recorded in detrital zircons from metasediments belonging to the Menderes massif (Kröner & Şengör 1990) and the Cycladic crystalline massif (Keay & Lister 2002). The upper intercept ages reported here are also largely compatible with ages reported from metagranites of the Menderes Massif (*c*. 2555–1740 Ma, single Pb–Pb zircon evaporation; Reischmann *et al*. 1991)

Late Palaeozoic tectonothermal event

Two orthogneiss samples, which were selected for U–Pb zircon dating, yielded concordant zircon ages ranging from 324 to 323 Ma. One sample yielded a lower intercept age at 320 ± 1.2 Ma. These ages are interpreted to date magma emplacement and provide the first reliable evidence for Carboniferous magmatic activity within the pre-Alpine basement of the External Hellenides. The Carboniferous igneous event on Kithira seems to be synchronous with the Carboniferous amphibolite-facies metamorphic event (*c*. 330 Ma) that has recently been determined for the basement rocks of eastern Crete (Finger *et al*. 2002; Romano *et al*. 2004). Moreover, the new data may indicate that the post-Carboniferous metamorphic events within the External Hellenides, that is, the Permian (*c*. 260 Ma) amphibolite-facies metamorphism (e.g. Finger *et al*. 2002) and the Alpine HP–LT metamorphic event, had only minor or no impact on the U–Pb isotopic system of the investigated zircons.

Carboniferous intrusion ages have also been determined for igneous and metaigneous rocks situated within other crystalline pre-Alpine complexes of the Aegean region (Table 2). The Kastoria Granite within the basement of the Pelagonian zone in NW Greece (Fig. 1) yielded a Late Carboniferous age (302 ± 5 Ma, U–Pb on zircon; Mountrakis 1984). The Granitoid Complex of Pieria area (Fig. 1) yielded 302 ± 5 Ma (U–Pb on zircon; Yarwood & Aftalion 1976). The granitic orthogneisses of NW and central Evia yielded 308–319 Ma (U–Pb on zircon; De Bono 1998). In the Cycladic crystalline basement, zircon geochronology of orthogneiss from Syros, Paros, Naxos and Samos islands (Fig. 1, Table 2) yielded ages of 328–315 Ma (U–Pb on zircon; Tomaschek *et al*. 2000), 317 ± 2 Ma (Pb–Pb on zircon; Engel & Reischmann 1998), 322–306 Ma (U–Pb on zircon; Keay *et al*. 2001; Pb–Pb on zircon; Reischmann 1998) and 302 Ma (Pb–Pb on zircon; Ring *et al*. 1999*b*), respectively. These Carboniferous ages are considered to reflect the timing of the crystallization of the igneous protolith of these gneisses. Evidence for Carboniferous plutonism has also been reported from the Rhodope massif in Bulgaria (311–300 Ma, U–Pb on zircon; e.g. Peytcheva *et al*. 2004) and Greece (294 ± 8 Ma, U–Pb on zircon; Liati & Gebauer 1999), the Strandja massif (309 ± 24 Ma, Pb–Pb on zircon; Okay *et al*. 2001) and the Sakarya zone in NW Turkey (313–293 Ma, Pb–Pb on zircon; Özmen & Reischmann 1999) (Fig. 1; Table 2).

From the above-mentioned data it is obvious that the igneous event on Kithira reflects the initial stage of Late Carboniferous igneous activity within the pre-Alpine continental fragments of the Aegean region. The entire period of magmatic activity lasted *c*. 25 Ma (*c*. 325–300 Ma). Most Aegean Carboniferous granitoids have generally similar geochemical and isotope characteristics (Pe-Piper & Piper 2002), suggesting that during the Late Carboniferous the pre-Alpine basement of the External Hellenides was in close proximity to the Cycladic and Pelagonian basements and to the continental fragments of NE Greece and NW Turkey. The majority of the Aegean continental fragments also show clear evidence of Neoproterozoic to Cambrian magmatic events, which should be related to the Cadomian (Pan-African) cycle at the northern margin of Gondwana (Table 2). Moreover, apart from the Carboniferous event, the above-mentioned pre-Alpine crustal blocks as well as the Menderes

Table 2. *Age data for pre-Jurassic tectonothermal events in the Aegean region and vicinity*

Locality	Age (Ma)	Methods	Source
Cimmerian blocks			
Strandja massif	309 ± 24; *308 ± 16*; *c*. 271	Pb–Pb: zrn	Okay *et al*. (1996, 2001)
Sakarya zone	313–293	U–Pb: zrn	Özmen & Reischmann (1999)
Istanbul zone	590–560	U–Pb; Pb–Pb: zrn	Chen *et al*. (2002)
Rhodope massif			
Bulgaria	311 ± 5; 300 ± 11	U–Pb: zrn	Peytcheva *et al*. (2004)
NE Greece	294 ± 8	U–Pb: zrn	Liati & Gebauer (1999)
Pelagonian zone			
Florina	*c*. 690	U–Pb; Pb–Pb: zrn	Anders *et al*. (2003)
Kastoria	302 ± 5	U–Pb: zrn	Mountrakis (1984)
Pieria	302 ± 5	U–Pb: zrn	Yarwood & Aftalion (1976)
Mt. Olympos	280–290	Pb–Pb zrn	Reischmann *et al*. (2001)
Evia	308–319	U–Pb: zrn	De Bono (1998); Vavassis *et al*. (2000)
Cycladic massif			
Paros	317 ± 2	Pb–Pb: zrn	Engel & Reischmann (1998)
Naxos	316 ± 4; 322–306; 275 ± 3; 233 ± 2	Pb–Pb: zrn; U–Pb	Reischmann (1998); Keay *et al*. (2001)
Syros	328 ± 4; 315 ± 3; 242 ± 3	U–Pb: zrn	Tomaschek *et al*. (2000)
Samos	302; 230–240	Pb–Pb: zrn	Ring *et al*. (1999*b*); Ring & Layer (2003)
Ios	*c*. 500, *c*. *300*	Rb–Sr, U–Pb: zrn	Henjes-Kunst & Kreuzer (1982)
Entire belt	pre-400, peaks at *c*. 550, *c*. 650	U–Pb: zrn	Keay & Lister (2002)
External Hellenides			
E. Crete	511 ± 16; 514 ± 14; *c*. *330*; c. *260*, 223 ± 3	Th–U–Pb: mz; U–Pb: zrn	Finger *et al*. (2002); Romano *et al*. (2004)
Kithira	324 ± 2; 323 ± 3	U–Pb: zrn	This study
Menderes massif			
Ödemis submassif	551 ± 1.4; 246–235	U–Pb; Pb–Pb: zrn	Hetzel *et al*. (1998); Koralay *et al*. (2001)
Cine submassif	657 ± 1.4; *c*. 550; 566 ± 9; 541 ± 14	U–Pb; Pb–Pb: zrn	Loos & Reischmann (1999); Gessner *et al*. (2004)
Entire Anatolide belt	2555–1740	Pb–Pb: zrn	Reischmann *et al*. (1991)
Gondwana			
Arabian–Nubian Shield	pre-529	U–Pb: zrn; Rb–Sr; K–Ar	Halpern & Tristan (1981); Ayalon *et al*. (1987); Moghazi (1999)
Hoggar massif (Algeria)	pre-530	Rb–Sr; K–Ar; U–Pb: zrn	Cheilletz *et al*. (1992); Black *et al*. (1994); Paquette *et al*. (1998)

Age data in italics are for metamorphic events; those in normal typeface are for an igneous event; zrn, zircon; mz, monazite.

massif, where no Carboniferous granites have been found so far, have been further overprinted by Permo-Triassic (Table 2) and Alpine orogenic imprints (e.g. Liati & Gebauer 1999; Ring & Layer 2003, and references therein). As the pre-Alpine Aegean crustal blocks shared almost the same post-Neoproterozoic geological evolution, it is reasonable to assume that in Neoproterozoic times they were juxtaposed along the same margin of northern Gondwana. Given that the major domains of northern Gondwana, such as the West African Craton and the Arabian–Nubian Shield in Sinai, are free from post-Cambrian orogenic events (Table 2), it is suggested that the pre-Alpine basement of the External Hellenides and the adjacent continental blocks were parts of the Gondwana-derived Cimmerian terrane.

The geodynamic setting of the Carboniferous granitoids of Kithira is still an open question. Most Aegean Carboniferous plutons are geochemically classified as granodiorites and granites (Pe-Piper & Piper 2002). They are peraluminous and display similarities to I- and S-type granites, indicating that plutonism was probably produced during a subduction process (e.g. Reischmann *et al*. 2001; Peytcheva *et al*. 2004). Some current models (e.g. Stampfli 2000; Vavassis *et al*. 2000) describe Late Carboniferous granitoids as remnants of a magmatic arc (Variscan) in the southern active margin of Eurasia resulting from northward subduction of Palaeotethys lithosphere. However, the results on the post-Cambrian evolution of the Aegean blocks presented above imply that such models should be re-examined. From the above compilation of data it seems that the Carboniferous origin of granitoids in the Aegean region occurred between 325 and 300 Ma. The spatial and temporal distribution of these rocks indicates a general younging trend from southwestern Greece (Kithira) towards northern Greece and Turkey (Fig. 8). This trend seems to be compatible with palaeogeographical models, which suggest southward subduction of Palaeotethys lithosphere beneath the marginal fragments of northern Gondwana (Cimmerian blocks) during the Late Palaeozoic (e.g. Şengör *et al*. 1984; Kotopouli *et al*. 2000). Probably, the northward shift of magmatic activity in the upper plate (Gondwana; Fig. 8b) was associated with Late Carboniferous accretion of microplates and a northeastward retreat of the cold and dense oceanic slab of the Palaeotethys as a result of subduction rollback. Further evidence for Carboniferous north-verging structures in basement rocks of northern Gondwana has been found on Crete, where the mylonitic foliation of deformed Cambrian granitoids results from Carboniferous (*c*. 330 Ma) amphibolite-facies top-to-the-north shearing (Finger *et al*. 2002; Romano *et al*. 2004).

Orogens that are controlled by subduction rollback may be subjected to rifting in the back-arc region and switches from crustal shortening and extension (e.g. Royden 1993; Faccenna *et al*. 2001). The presence of Late Carboniferous and Early Permian hemipelagic sediments in rift sequences of the External Hellenides (Phyllite–Quartzite unit; Krahl *et al*. 1983) and the Cyclades (Makrotantalos unit in Andros; Papanikolaou 1979), respectively, is compatible with the formation of marine basins in the back-arc region. During this persistent subduction process, rifting was probably followed by a subsequent compressional event, which is indicated by Scythian conglomerates (Krahl *et al*. 1983).

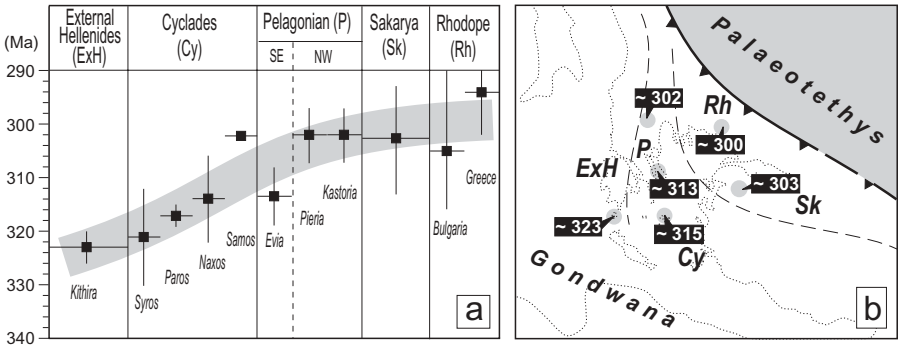

Fig. 8. (**a**) Compilation of U–Pb and Pb–Pb zircon ages for the Aegean Carboniferous plutonic rocks, showing a general younging trend from southwestern Greece (Kithira) towards northern Greece and Turkey. Locations and age data are given in Figure 1 and Table 2, respectively. (**b**) Map showing the spatial and temporal distribution of the Aegean Late Carboniferous plutonic rocks. The distribution suggests southward subduction of Palaeotethys lithosphere beneath the marginal fragments of northern Gondwana (Cimmerian blocks) during the Late Palaeozoic. The Late Palaeozoic palaeogeographical reconstruction of the Eastern Mediterranean region is after Şengör *et al*. (1984).

Conclusions

U–Pb data on zircon of granitic orthogneiss of Kithira island record a Late Carboniferous (324–323 Ma) magmatic event occurring within the pre-Alpine basement of the External Hellenides. Ages of inherited zircons in gneiss imply that the basement rocks of the External Hellenides were possibly derived from Late Archaean–Early Proterozoic crustal material. The new ages, in combination with published geochronogical data from other Aegean crustal fragments, provide further evidence of a temporally restricted period of plutonism in the pre-Alpine Aegean region around 325–300 Ma. The spatial and temporal distribution of Carboniferous Aegean plutons implies that this plutonism occurred during southward subduction of Palaeotethys lithosphere beneath the marginal fragments of Gondwana. Moreover, the Hellenic basement generally has a common post-Neoproterozoic tectonothermal history with adjacent crystalline complexes and especially with the Cyclades. Based on these similarities, it seems that the basement of the External Hellenides together with the Cycladic and Pelagonian basements and the continental fragments of NE Greece and NW Turkey, as well as the Menderes massif, were parts of the Gondwana-derived Cimmerian terrane.

The authors gratefully acknowledge the editing assistance of M. Whitehouse and constructive reviews by P. Hoskin and U. Ring. P. X. acknowledges discussions with C. Katagas (Patras) for the geology of Kithira. Thanks are due to S. Romano (Universität Frankfurt a.M.) for her assistance with CL images. This work was financially supported by a common grant of IKY (Greek State Scholarships Foundation) and DAAD (IKYDA program 2004, grant D/02/28640).

References

Anders, B., Reischmann, T., Poller, U. & Kostopoulos, D. 2003. The oldest rocks in Greece: geochronological evidence for remnants of a Precambrian basement within the central Hellenides. *Geochimica et Cosmochimica Acta*, **67**, A18.

Ayalon, A., Steinitz, G. & Starinsky, A. 1987. K–Ar and Rb–Sr whole rock ages reset during Pan-African event in the Sinai Peninsula (Ataqua area). *Precambrian Research*, **37**, 191–197.

Black, R., Latouche, L., Liégeois, J.P., Caby, R. & Bertrand, J.M. 1994. Pan-African displaced terranes in the Tuareg shield (Central Sahara). *Geology*, **22**, 641–644.

Cheilletz, A., Bertrand, J.M. & Charoy, B. *et al.* 1992. Geochemistry and geochronology Rb–Sr, K–Rr and $^{40}Ar/^{39}Ar$ of the pan-African granitic complexes of the Tamanrasset area (Algeria)—relationships with the associated Sn–W mineralizations and tectonic evolution of central Hoggar. *Bulletin de la Société Géologique de France*, **163**, 733–750.

Chen, F., Siebel, W., Satir, M., Terzioğlu, M.N. & Saka, K. 2002. Geochronology of the Karadere basement (NW Turkey) and implications for the geological evolution of the Istanbul zone. *International Journal of Earth Science*, **91**, 469–481.

Corfu, F., Hanchar, J.M., Hoskin, P.W.O. & Kinny, P. 2003. An atlas of zircon textures. *In:* Hanchar, J.M. & Hoskin, P.W.O. (eds) *Zircon*. Mineralogical Society of America, Reviews in Mineralogy and Geochemistry, **53**, 469–500.

De Bono, A. 1998. *Pelagonian margins in central Evia island (Greece). Stratigraphy and geodynamic evolution*. PhD thesis, University of Lausanne.

Dercourt, J., Zonenshain, L.P. & Ricou, L.E. *et al.* 1986. Geological evolution of the Tethys belt from the Atlantic to the Pamirs since the Lias. *Tectonophysics*, **123**, 241–315.

Dörr, W., Zulauf, G., Fiala, J., Franke, W. & Vejnar, Z. 2002. Neoproterozoic to Early Cambrian history of an active plate margin in the Tepla–Barrandian unit—a correlation of U–Pb isotopic-dilution-TIMS ages (Bohemia, Czech Republic). *Tectonophysics*, **352**, 65–85.

Doutsos, T., Piper, G., Boronkay, K. & Koukouvelas, I. 1993. Kinematics of the Central Hellenides. *Tectonics*, **12**, 936–953.

Engel, M. & Reischmann, T. 1998. Single zircon geochronology of orthogneisses from Paros, Greece. *Bulletin of the Geological Society of Greece*, **32**, 91–99.

Facenna, C. 2001. Cited in text.

Faccenna, C., Becker, T.W., Lucente, F.P., Jolivet, L. & Rosseti, F. 2001. History of subduction and back-arc extension in the Central Mediterranean. *Geophysical Journal International*, **145**, 809–820.

Finger, F., Krenn, E., Riegler, G., Romano, S. & Zulauf, G. 2002. Resolving Cambrian, Carboniferous, Permian and Alpine monazite generations in the polymetamorphic basement of eastern Crete (Greece) by means of the electron microprobe. *Terra Nova*, **14**, 233–240.

Franz, L. 1992. *Die polymetamorphe Entwicklung des Altkristallins auf Kreta und Dodekanes (Griechenland)*. Ferdinand Enke, Stuttgart.

Gessner, K., Collins, A., Ring, U. & Güngör, T. 2004. Structural and thermal history of poly-orogenic basement: U–Pb geochronology in the southern Menderes Massif, Western Turkey. *Journal of the Geological Society, London*, **161**, 93–101.

Halpern, M. & Tristan, N. 1981. Geochronology of the Arabian–Nubian Shield in southern Israel and eastern Sinai. *Journal of Geology*, **89**, 639–648.

Henjes-Kunst, F. & Kreuzer, H. 1982. Isotopic dating of pre-alpidic rocks from the island of Ios (Cyclades, Greece). *Contributions to Mineralogy and Petrology*, **80**, 245–253.

Hetzel, R., Romer, R.L., Candan, O. & Passchier, C.W. 1998. Geology of the Bozdag area, central Menderes Massif, SW Turkey: Pan-African basement and Alpine deformation. *Geologische Rundschau*, **87**, 394–406.

Jaffey, A.H., Flynn, K.F., Glendenin, L.E., Bentley, W.C. & Essling, A.M. 1971. Precision measurements of half-lives and specific activities of ^{235}U and ^{238}U. *Physical Review, Section C, Nuclear Physics*, **4**, 1889–1906.

Keay, S. & Lister, G. 2002. African provenance for the metasediments and metaigneous rocks of the Cyclades, Aegean Sea, Greece. *Geology*, **30**, 235–238.

Keay, S., Lister, G. & Buick, I. 2001. The timing of partial melting, Barrovian metamorphism and granite intrusion in the Naxos metamorphic core complex, Cyclades, Aegean Sea, Greece. *Tectonophysics*, **342**, 275–312.

Koralay, O.E., Satir, M. & Dora, O.O. 2001. Geochemical and geochronological evidence for Early Triassic calc-alkaline magmatism in the Menderes Massif, western Turkey. *International Journal of Earth Science*, **89**, 822–835.

Kotopouli, C., Pe-Piper, G. & Piper, D.J.W. 2000. Petrology and evolution of the

Hercynian Pieria Granitoid Complex (Thessaly, Greece): paleogeographic and geodynamic implications. *Lithos*, **50**, 137–152.

Krahl, J., Kauffmann, G., Kozur, H., Richter, D., Forster, O. & Heinritzi, F. 1983. Neue Daten zur Biostratigraphie and zur tektonischen Lagerung der Phyllit-Gruppe und der Trypali-Gruppe auf der Insel Kreta (Griechenland). *Geologische Rundschau*, **72**, 1147–1166.

Krogh, T.E. 1973. A low contamination method for hydrothermal decomposition of zircon and extraction of U and Pb for isotopic age determinations. *Geochimica et Cosmochimica Acta*, **37**, 485–494.

Kröner, A. & Şengör, A.M.C. 1990. Archean and Proterozoic ancestry in late Precambrian to early Paleozoic crustal elements of southern Turkey as revealed by single-zircon dating. *Geology*, **18**, 1186–1190.

Liati, A. & Gebauer, D. 1999. Constraining the prograde and retrograde *P–T–t* path of Eocene HP rocks by SHRIMP dating of different zircon domains: inferred rates of heating, burial, cooling and exhumation for central Rhodope, northern Greece. *Contributions to Mineralogy and Petrology*, **135**, 340–354.

Loos, S. & Reischmann, T. 1999. The evolution of the southern Menderes Massif in SW Turkey as revealed by zircon dating. *Journal of the Geological Society, London*, **156**, 1021–1030.

Ludwig, K.R. 1980. Calculation of uncertainties of U–Pb isotope data. *Earth and Planetary Science Letters*, **46**, 212–220.

Ludwig, K.R. 1988. *PbDat for MS-DOS: a computer program for IBM-PC compatibles for processing raw Pb-U-Th isotope data*. US Geological Survey open-file Report **88-542**.

Ludwig, K.R. 2001. *Isoplot/Ex—a geochronological toolkit for Microsoft Excel*. Berkeley Geochronological Center, Special Publications, **1a**.

Moghazi, A.M. 1999. Magma source and evolution of the late Neoproterozoic granitoids in the Gabal El Urf area, Eastern Desert, Egypt: geochemical and Sr–Nd isotopic constraints. *Geological Magazine*, **136**, 285–300.

Mountrakis, D. 1984. Structural evolution of the Pelagonia zone in northwestern Macedonia, Greece. *In:* Dixon, J.E. & Robertson, A.H.F. (eds) *The Geological Evolution of the Eastern Mediterranean*. Geological Society, London, Special Publications, **17**, 581–590.

Mountrakis, D. 1986. The Pelagonian zone in Greece: a polyphase-deformed fragment of the Cimmerian continent and its role in the geotectonic evolution of the eastern Mediterranean. *Journal of Geology*, **94**, 335–347.

Okay, A.I., Satir, M., Maluski, H., Siyako, M., Monie, P., Metzger, R. & Akyüz, S. 1996. Paleo- and Neo-Tethyan events in northwestern Turkey: geologic and geochronologic constraints. *In:* Yin, A. & Harrison, M. (eds) *The Tectonic Evolution of Asia*. Cambridge University Press, Cambridge, 420–441.

Okay, A.I., Satir, M., Tüyzüz, O., Akyüz, S. & Chen, F. 2001. The tectonics of the Strandja Massif: late-Variscan and mid-Mesozoic deformation and metamorphism in the northern Aegean. *International Journal of Earth Science*, **90**, 217–233.

Özmen, F. & Reischmann, T. 1999. The age of Sakarya continent in W. Anatolia: implication for the evolution of the Aegean region. *Journal of Conference Abstracts*, **4**, 805–806.

Papanikolaou, D. 1979. Contribution to the geology of the Aegean Sea: the island of Andros. *Annales Géologiques des Pays Helléniques*, **29**, 477–553.

Paquette, J.L., Caby, R., Djouadi, M.T. & Bouchez, J.L. 1998. U–Pb dating of the end of the Pan-African orogeny in the Tuareg shield: the post-collisional syn-shear Tioueine pluton (Western Hoggar, Algeria). *Lithos*, **45**, 245–253.

Pe-Piper, G. 1982. Geochemistry, tectonic setting and metamorphism of mid-Triassic volcanic rocks of Greece. *Tectonophysics*, **85**, 253–272.

Pe-Piper, G. & Piper, D.J.W. 2002. *The Igneous Rocks of Greece*. Borntträeger, Stuttgart.

Peytcheva, I., von Quadt, A. & Ovtcharova, M. *et al.* 2004. Metagranitoids from the eastern part of the Central Rhodopean Dome (Bulgaria): U–Pb, Rb–Sr and $^{40}Ar/^{39}Ar$ timing of emplacement and exhumation and isotope-geochemical features. *Contributions to Mineralogy and Petrology*, **82**, 1–31.

Poller, U., Liebetrau, V. & Todt, W. 1997. U–Pb single-zircon dating under cathodoluminescence control (CLC-method): application to polymetamorphic orthogneisses. *Chemical Geology*, **139**, 287–297.

Pupin, J.P. 1980. Zircon and granite petrology. *Contributions to Mineralogy and Petrology*, **73**, 207–220.

Reischmann, T. 1998. Pre-Alpine origin of tectonic units from the metamorphic complex of Naxos, Greece, identified by single zircon Pb/Pb dating. *Bulletin of the Geological Society of Greece*, **32**, 101–111.

Reischmann, T., Kröner, A., Todt, W., Dürr, S. & Şengör, A.M.C. 1991. Episodes of crustal growth in the Menderes Massif, W Turkey, inferred from zircon dating. *Terra Abstracts*, **3**, 34.

Reischmann, T., Kostopoulos, D.K., Loss, S., Anders, B., Avgerinas, A. & Sklavounos, S.A. 2001. Late Palaezoic magmatism in the basement rocks southwest of Mt. Olympos, central Pelagonian zone, Greece: remnants of a Permo-Carboniferous magmatic arc. *Bulletin of the Geological Society of Greece*, **34**, 985–993.

Ring, U. & Layer, P.W. 2003. High-pressure metamorphism in the Aegean, eastern Mediterranean: underplating and exhumation from the Late Cretaceous until the Miocene to Recent above the retreating Hellenic subduction zone. *Tectonics*, **23**(1022), doi: 10.1029/2001TC001350.

Ring, U., Gessner, K., Güngör, T. & Passchier, C.W. 1999a. The Menderes Massif of western Turkey and the Cycladic Massif in the Aegean—do they really correlate? *Journal of the Geological Society, London*, **156**, 3–6.

Ring, U., Laws, S. & Bernet, M. 1999b. Structural analysis of a complex nappe sequence and late-orogenic basins from the Aegean Island of Samos, Greece. *Journal of Structural Geology*, **21**, 1575–1601.

Robertson, A.H.F. & Dixon, J.E. 1984. Introduction: aspects of the geological evolution of the Eastern Mediterranean. *In:* Dixon, J.E. & Robertson, A.H.F. (eds) *The Geological Evolution of the Eastern Mediterranean*. Geological Society, London, Special Publications, **17**, 1–74.

Robertson, A.H.F., Clift, P.D., Degnan, P. & Jones, G. 1991. Palaeogeographic and palaeotectonic evolution of the Eastern Mediterranean Neotethys. *Palaeogeography, Palaeoclimatology, Palaeoecology*, **87**, 289–344.

Robertson, A.H.F., Dixon, J.E. & Brown, S. *et al.* 1996. Alternative tectonic models for the Late Palaeozoic–Early Tertiary development of Tethys in the Eastern Mediterranean region. *In:* Morris, A. & Tarling, D.H. *et al.* (eds) *Palaeomagnetism and Tectonics of the Mediterranean Region*. Geological Society, London, Special Publications, **105**, 239–263.

Romano, S.S., Dörr, W. & Zulauf, G. 2004. Cambrian granitoids in the pre-Alpine basement of Crete (Greece): evidence from U–Pb dating of zircon. *International Journal of Earth Science*, **93**, 844–859.

Royden, L.H. 1993. The tectonic expression of slab pull at continental convergent boundaries. *Tectonics*, **12**, 303–325.

Seidel, E. 1978. *Zur Petrologie der Phyllit–Quarzit-Serie Kretas*. Habilitation thesis, University of Braunschweig.

Seidel, E., Kreuzer, H. & Harre, W. 1982. A Late Oligocene/Early Miocene High Pressure Belt in the External Hellenides. *Geologisches Jahrbuch*, **E23**, 165–206.

Şengör, A.M.C., Yilmaz, Y. & Sungurlu, O. 1984. Tectonics of the Mediterranean Cimmerides: nature and evolution of the western termination of Palaeo-Tethys. *In:* Dixon, J.E. & Robertson, A.H.F. (eds) *The Geological Evolution of the Eastern Mediterranean*. Geological Society, London, Special Publicationss, **17**, 77–112.

Stampfli, G.M. 2000. Tethyan oceans. *In:* Bozkurt, E., Winchester, J.A. & Piper, D.J.W. (eds) *Tectonics and Magmatism in Turkey and the Surrounding Area*. Geological Society, London, Special Publications, **173**, 163–185.

Stampfli, G.M. & Borel, G.D. 2002. A plate tectonic model for the Palaeozoic and Mesozoic constrained by dynamic plate boundaries and restored synthetic oceanic isochrones. *Earth and Planetary Science Letters*, **169**, 17–33.

Stampfli, G.M. & Mosar, J. 1999. The making and becoming of Apulia. *Memorie di Scienze Geologiche*, **51**, 141–154.

Steiger, R.H. & Jäger, E. 1977. Subcommission on geochronology: convention on the use of decay constants in geo- and cosmochronology. *Earth and Planetary Science Letters*, **36**, 359–362.

Theye, T., Seidel, E. & Vidal, O. 1992. Carpholite, sudoite and chloritoid in low-temperature high-pressure metapelites from Crete and the Peloponnese, Greece. *European Journal of Mineralogy*, **4**, 487–507.

Tomaschek, F., Kennedy, A., Keay, S. & Ballhaus, C. 2000. U/Pb-SHRIMP results for zircons from Syros, Greece: geochronological constraints on Carboniferous and Triassic magmatic episodes in the Cyclades. *Terra Nostra*, **2000/5**, 58.

Vavassis, I., De Bono, A., Stampfli, G.M., Giorgis, D., Valloton, A. & Amelin, Y. 2000. U–Pb and Ar–Ar geochronological data from Pelagonian basement in Evia (Greece): geodynamic implications for the evolution of the Paleotethys. *Schweizerische Mineralogische und Petrographische Mitteilungen*, **80**, 21–43.

Xypolias, P. & Doutsos, T. 2000. Kinematics of rock flow in a crustal-scale shear zone: implication for the orogenic evolution of the southwestern Hellenides. *Geological Magazine*, **137**, 81–96.

Xypolias, P. & Koukouvelas, I. 2001. Kinematic vorticity and strain rate patterns associated with ductile extrusion in the Chelmos Shear zone (External Hellenides, Greece). *Tectonophysics*, **338**, 59–77.

Yarwood, G.A. & Aftalion, M. 1976. Field relations and U–Pb geochronology of a granite from the Pelagonian zone of the Hellenides (High Pieria, Greece). *Bulletin de la Société Géologique de France*, **18**, 259–264.

Received 6 September 2004; revised typescript accepted 23 March 2005.
Scientific editing by Martin Whitehouse